

應用在無線通訊的低雜訊高電子遷移率電晶體之線性度的

研究與改善

研究生：林岳欽

指導教授：張翼 博士

國立交通大學材料科學與工程研究所

摘要

這篇論文為研究高電子遷移率電晶體(HEMT)之線性度的改善，此研究首先分析三次交互調變失真(IM3)及三次交叉點(IP3)與轉導值(transconductance)之間的關係，由所推導的結果得知，越平坦的轉導分布圖形之元件的線性度越好，因此本研究分四大部分去探討元件線性度的改善。

首先，我們研究利用複合通道層(composite channel)的變形高電子遷移率電晶體(MHEMT)，來發展低雜訊暨高線性度之元件，此研究主要是利用複合通道層能提升電子在通道層的侷限能力進而提升元件之線性度。接著我們研究均勻性摻雜(uniformly doped)與平面性摻雜(planer doped)對元件線性度的影響，本研究驗證均勻性摻雜之變形高電子遷移率電晶體雖然具有較低之最高轉導值，但其轉導值之分布較為平坦，故線性度亦較佳。

對於假形高電子遷移率電晶體(PHEMT)，首先我們發展出以砷化鋁鎵(AlGaAs)為 spacer 的磷化銦鎵/砷化銦鎵(InGaP/InGaAs) 假形高電子遷移率電晶體，由於利用磷化銦鎵為蕭特基層(Schottky layer)可降低元件閘極(Gate)之漏電流及砷化鋁鎵(AlGaAs)為 spacer 可提升元件之電子遷移率(mobility)，因此此元件具有低雜訊及高線性度之特性。

最後我們研究利用額外的電子摻雜，來提升元件的線性度。此研究是以一般

平面性摻雜的磷化銦鎵/砷化銦鎵元件為基準，分別額外的摻雜電子在蕭特基層及通道層，探討額外的電子摻雜在不同層時對元件線性度的影響。最後驗證出額外摻雜電子在元件上會使得元件之最大轉導值下降，但其分布會更為平坦，而使得元件之線性度提升。接著提升偏壓條件，對額外摻雜在通道層及蕭特基層做適用是測試，最後亦驗證得額外摻雜在通道層有較佳的線性度。



Linearity Improvement of Low Noise HEMT for Wireless Communication Applications

Student: Yueh-Chin Lin

Advisor: Dr. Edward Yi Chang

Department of Materials Science and Engineering

National Chiao Tung University

Abstract

In this paper, high-electron-mobility transistors (HEMTs) with doping profile modification are discussed for device linearity improvement. The modification was based on the third-order intermodulation distortion (IM3) and the third-order intercept point (IP3) analysis through simple equivalent circuit of the devices. The correlation of the extrinsic transconductance (G_m) with IM3 and IP3 indicates that flatter G_m distribution vs gate bias voltage causes lower IM3 level and that high G_m with flatter G_m distribution result in higher IP3 of the devices. Therefore, doping modification that improves the flatness of the G_m distribution will improve the device linearity.

The study is divided into four parts: First, a metamorphic high-electron-mobility transistor (MHEMT) with $\text{In}_{0.55}\text{Ga}_{0.45}\text{As}/\text{In}_{0.67}\text{Ga}_{0.33}\text{As}/\text{In}_{0.55}\text{Ga}_{0.45}\text{As}$ composite channel layers was developed for low noise and high-linearity applications. The use of a composite channel results in high electron mobility and good confinement of electrons in the channel region which are the desired characteristics of a low-noise and high-linearity device. The device shows great potential for high-linearity and low-noise applications at high frequencies.

Second, the uniformly-doped and the δ doped $\text{In}_{0.52}\text{Al}_{0.48}\text{As}/\text{In}_{0.6}\text{Ga}_{0.4}\text{As}$ MHEMT were fabricated and the DC characteristics and the third-order intercept

point (IP₃) of these devices were measured and compared. Due to more uniform electron distribution in the quantum well region, the uniformly-doped MHEMT exhibits flatter G_m (transconductance) vs I_{DS} (drain to source current) curve and much better linearity with higher IP₃ and higher IP₃ to P_{DC} ratio as compared to the δ doped MHEMT, even though the δ doped device exhibits higher peak transconductance. As a result, the uniformly doped MHEMT is more suitable for communication systems that require high linearity operation.

Third, a low noise InGaP/InGaAs pseudomorphic high-electron-mobility transistors (PHEMTs) with high IP₃ was developed. The device utilizes InGaP as Schottky layer to achieve a low noise figure and uses AlGaAs as the spacer to improve the electron mobility and the device also uses dual delta doped layers for uniform electron distribution in the channel to improve the device linearity.

Finally, doping modification in the Schottky layer (Schottky layer doped) and in the channel layer (channel doped) of the conventional δ doped InGaP/InGaAs PHEMT were experimented to see the extra doping effect on the HEMT device linearity. DC and RF performances of these devices were measured and compared. It is found that extra doping either in the channel region or in the Schottky layer can improve the flatness of the G_m distribution under different gate bias conditions and thus achieve lower IM₃ and higher IP₃ of these devices with small scarification in the peak G_m value as compared to the conventional delta doped devices. The power performances of these devices were tested with different drain to source voltage (V_{DS}) bias points. When the V_{DS} bias was increased, the G_m values of the channel doped device and the Schottky layer doped device increased and decreased respectively with the increasing V_{DS} bias. The adjacent-channel power ratio (ACPR) measurements of these devices were performed at different DC bias power levels. Overall, it was found that channel doped device demonstrated best linearity performance among these three

different types of devices studied with highest IP3 level, lowest IM3 and best ACPR under CDMA modulation even though it has the lowest electron mobility among these devices. Overall, different structures and doping profiles of InGaP/InGaAs PHEMT and InAlGs/InGaAs MHEMT devices were experimented for device linearity improved. It's found with paper design of the device structure and doping profile, the linearity of the HEMT device can be greatly improved and the experimental results match well with the theoretical analysis in this thesis.



誌謝

由於許多人的幫忙，才使得本論文得以完成。首先要感謝我的指導教授張翼博士帶領我進入砷化鎵領域並提供足夠的儀器及完整的訓練使我能有如此難得的經驗能完成此砷化鎵高頻元件的研究；其次要感謝平山祥郎先生提供機會以及山口浩司先生的指導讓我更進一步的研究砷化鎵的磊晶，且能更完整了解砷化鎵高頻元件的發展。

另外我要感謝吳建華博士、張尚文博士與楊宗熿博士在實驗上的建議以及國家奈米實驗室(NDL)與交大半導體中心提供良好的儀器設備與環境，使實驗能夠順利進行。

我也要感謝實驗室的研究夥伴：陳冠吉同學、張信源同學、吳偉誠同學、吳雲驥同學、謝炎璋同學、黃瑞乾同學、黃珍嬋同學、張家達同學、莊蕙菁小姐與實驗室其他曾幫助過我的同學，因為你們的幫忙本論文才得以順利完成。

最後我要特別感謝我的家人，尤其是我的母親及姐姐的關心支持及鼓勵，使我無後顧之憂能夠專心的完成學業，願與你們分享這份榮耀。

Contents

Abstract (in Chinese)	i
Abstract (in English)	iii
Acknowledge (in Chinese)	vi
Contents	vii
Table Captions	x
Figure Captions	xi
Chapter 1 Introduction	1
Chapter 2 Device Linearity Analysis	5
2.1 Introduction.....	5
2.2 The nonlinear effects of device.....	5
2.2.1 Gain compression.....	5
2.2.2 Analysis of IM3 and IP3.....	6
2.3 Polynomial curve fitting technique.....	9
Chapter 3 Fabrication of High ElElectron Mobility Transistor	12
3.1 Introduction of HEMT process.....	12
3.2 MHEMT process.....	13
3.2.1 Device active region definition.....	13
3-2-2 Ohmic contact formation.....	14
3.2.3 Recess and gate formation.....	14
3.2.4 Device passivation.....	15
3-2-5 Air-bridge plating.....	16

3.3 InGaP PHEMT process.....	17
Chapter 4 A Low Noise Composite-Channel Metamorphic HEMT for Wireless Communication Applications.....	23
4.1 Introduction.....	23
4.2 Device performance.....	24
4.3 Conclusion.....	25
Chapter 5 Device Linearity Comparison of the Uniformly-Doped and the δ Doped $\text{In}_{0.52}\text{Al}_{0.48}\text{As}/\text{In}_{0.6}\text{Ga}_{0.4}\text{As}$ MHEMTs ..	32
5.1 Introduction.....	32
5.2 Results and discussion.....	33
5.3 Conclusion.....	34
Chapter 6 A Low Noise InGaP PHEMT with AlGaAs spacer for High IP3 Application	41
6.1 Introduction.....	41
6.2 Results and discussion.....	41
6.3 Conclusions.....	42
Chapter 7 The δ Doped InGaP/InGaAs PHEMTs with Doping Profile Modification for Device Linearity Improvement.....	49
7.1 Introduction.....	49
7.2 Device structure.....	50
7.3 Results and discussion.....	51
7.4 Conclusions.....	54

Chapter 8 Conclusions.....65
Reference.....67

Vita (in Chinese)

Publication List



Table Captions

Chapter 4

Table4-1 Performance of the $\text{In}_{0.67}\text{Ga}_{0.33}\text{As}$ composite-channel MHEMT and the $\text{In}_{0.6}\text{Ga}_{0.4}\text{As}$ conventional MHEMT of the $0.25 \times 160 \mu\text{m}^2$ devices.

Chapter 5

Table5-1 Comparison of the DC characteristics of the Uniform-doped and the δ doped $\text{In}_{0.52}\text{Al}_{0.48}\text{As}/\text{In}_{0.6}\text{Ga}_{0.4}\text{As}$ MHEMTs.

Table5-2 Comparison of the IM3 and IP3 of the Uniformly-doped and δ doped $\text{In}_{0.52}\text{Al}_{0.48}\text{As}/\text{In}_{0.6}\text{Ga}_{0.4}\text{As}$ MHEMTs.



Chapter 6

Table 6-1 Comparison noise figure and IP3 with AlGaAs/InGaAs PHEMT.

Chapter 7

Table 7-1 Comparison of the DC characteristics of the three different types of devices.

Table 7-2 Comparison of the IM3 and IP3 of the three different types of devices.

Table 7-3 $P_{1\text{dB}}$, Gain, PAE and ACPR of the three different devices under different V_{DS} at class AB bias.

Figure Captions

Chapter 1

Figure 1-1 The band diagram of the InGaP/InGaAs PHEMT.

Chapter 2

Figure 2-1 Output power spectrum of the two-tone input signal.

Figure 2-2 A simple equivalent circuit of device.

Chapter 3

Figure 3-1 Process flow of the InGaP PHEMT :

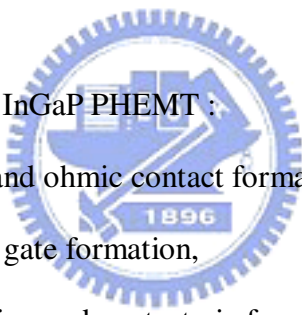
- 
- (a) Mesa isolation and ohmic contact formation,
 - (b) Gate recess and gate formation,
 - (c) Device passivation and contact via formation, and
 - (d) air-bridge plating.

Figure 3-2 The SEM image of the T-shaped gate.

Figure 3-3 The major steps of air-bridge formation.

Figure 3-4 The Image of the finished $0.25 \times 160 \mu\text{m}^2$ HEMT device

Chapter 4

Figure 4-1 (a) Structure of $\text{In}_{0.67}\text{Ga}_{0.33}\text{As}$ composite-channel MHEMT.

(b) Structure of $\text{In}_{0.6}\text{Ga}_{0.4}\text{As}$ conventional MHEMT.

Figure 4-2 (a) I-V characteristics, (b) Extrinsic transconductances vs gate bias of the $0.25 \times 160 \mu\text{m}^2$ $\text{In}_{0.67}\text{Ga}_{0.33}\text{As}$ composite-channel MHEMT.

Figure 4-3 The gate to drain breakdown voltage of the $0.25 \times 160 \mu\text{m}^2$ $\text{In}_{0.67}\text{Ga}_{0.33}\text{As}$ composite-channel MHEMT.

Figure 4-4 Extrinsic transconductances of the $\text{In}_{0.67}\text{Ga}_{0.33}\text{As}$ composite-channel MHEMT and the $\text{In}_{0.6}\text{Ga}_{0.4}\text{As}$ conventional MHEMT of the $0.25 \times 160 \mu\text{m}^2$ devices.

Figure 4-5 Noise and associated gain of the composite-channel MHEMT at $V_{\text{DS}} = 1.5 \text{ V}$ and $I_{\text{DS}} = 50 \text{ mA/mm}$.

Chapter 5

Figure 5-1 Structure of the $\text{In}_{0.52}\text{Al}_{0.48}\text{As}/\text{In}_{0.6}\text{Ga}_{0.4}\text{As}$ MHEMT :

(a) Uniformly-doped, (b) δ doped.

Figure 5-2 Drain to source current (I_{DS}) vs gate to source voltage (V_{GS}) of the $0.3 \times 160 \mu\text{m}^2$ $\text{In}_{0.52}\text{Al}_{0.48}\text{As}/\text{In}_{0.6}\text{Ga}_{0.4}\text{As}$ MHEMT devices.

Figure 5-3 Extrinsic transconductance (G_{m}) vs drain to source current (I_{DS}) of the $0.3 \times 160 \mu\text{m}^2$ $\text{In}_{0.6}\text{Ga}_{0.4}\text{As}$ MHEMT devices.

Figure 5-4 Comparison of device linearity of the uniformly-doped and the δ doped $\text{In}_{0.52}\text{Al}_{0.48}\text{As}/\text{In}_{0.6}\text{Ga}_{0.4}\text{As}$ MHEMTs.

Chapter 6

Figure 6-1 Structure of $\text{InGaP}/\text{AlGaAs}/\text{InGaAs}$ PHEMT.

Figure 6-2 The $0.25 \times 160 \mu\text{m}^2$ $\text{InGaP}/\text{AlGaAs}/\text{InGaAs}$ PHEMT DC characteristics:

(a) I-V characteristics, (b) Transconductance vs V_{GS} and I_{DS} curves.

Figure 6-3 The Drain to Gate breakdown voltage of the $0.25 \times 160 \mu\text{m}^2$ $\text{InGaP}/\text{AlGaAs}/\text{InGaAs}$ PHEMT device.

Figure 6-4 Measured Third-Order Products and Fundamental Power of a $0.25 \times 300\text{-}\mu\text{m}^2$ InGaP/AlGaAs/InGaAs PHEMT.

Figure 6-5 InGaP/AlGaAs/InGaAs PHEMT Gate leakage current.

Chapter 7

Figure 7-1 Structures of the three InGaP/InGaAs PHEMTs in this study :

- (a) δ -doped device, (b) Lightly channel doped PHEMT, and
- (c) Schottky layer doped

Figure 7-2 (a) Extrinsic transconductance (G_m) vs V_{GS} curve, (b) I_{DS} vs V_{GS} curves for the three different types of devices studied, the device size is $0.25 \times 160\text{-}\mu\text{m}^2$ and V_{DS} bias is 1.5V.

Figure 7-3 IP_3 vs. I_{DS} curves of the three $0.25 \times 160\text{-}\mu\text{m}^2$ InGaP/InGaAs PHEMTs in this study, the test frequency is 5.8GHz and $V_{DS} = 1.5\text{V}$.

Figure 7-4 IM_3 vs. power backed off from P_{1dB} curve for the three different types of InGaP/InGaAs PHEMTs (device size: $0.25 \times 160\text{-}\mu\text{m}^2$) when $V_{DS} = 1.5\text{V}$, I_{DS} bias at maximum IP_3 and the input signal frequency is 5.8GHz

Figure 7-5 Extrinsic transconductance (G_m) vs V_{GS} curve with different V_{DS} bias points: (a) The Schottky doped layer device, (b) The channel doped device.

Figure 7-6 ACPR spectrum of the InGaP/InGaAs PHEMTs (device size: $0.25 \times 160\text{-}\mu\text{m}^2$) with $V_{DS} = 3\text{V}$, class AB bias and the input signal frequency is 5.8GHz: (a) The Schottky layer doped device,
(b) The channel doped device.